OPEN ACCESS

Environment & Ecology ARTICLE

Organic carbon loss from the black soil region threatens food security in China

Jian Chen,[1,2,8] Wenyou Hu,[1,2,8,*] Xianghua Xu,[3] Yuxin Tong,[4] Guojing Yan,[1,2] Dongsheng Yu,[1,2] Yuguo Zhao,[1,2] Lixia Ma,[1,2] Enze Xie,[1,2] Yu Zhang,[1,2] Tingrun Zou,[1,2] Zhongjun Jia,[5] Michael L. Thompson,[6] Miguel Angel Taboada,[7] and Yongcun Zhao[1,2,*]

*Correspondence: yczhao@issas.ac.cn (Y.C.); wyhu@issas.ac.cn (W.H.)

Received: September 15, 2025; Accepted: March 10, 2026; Published Online: March 16, 2026; https://doi.org/10.59717/j.xinn-geo.2026.100213

GRAPHICAL ABSTRACT

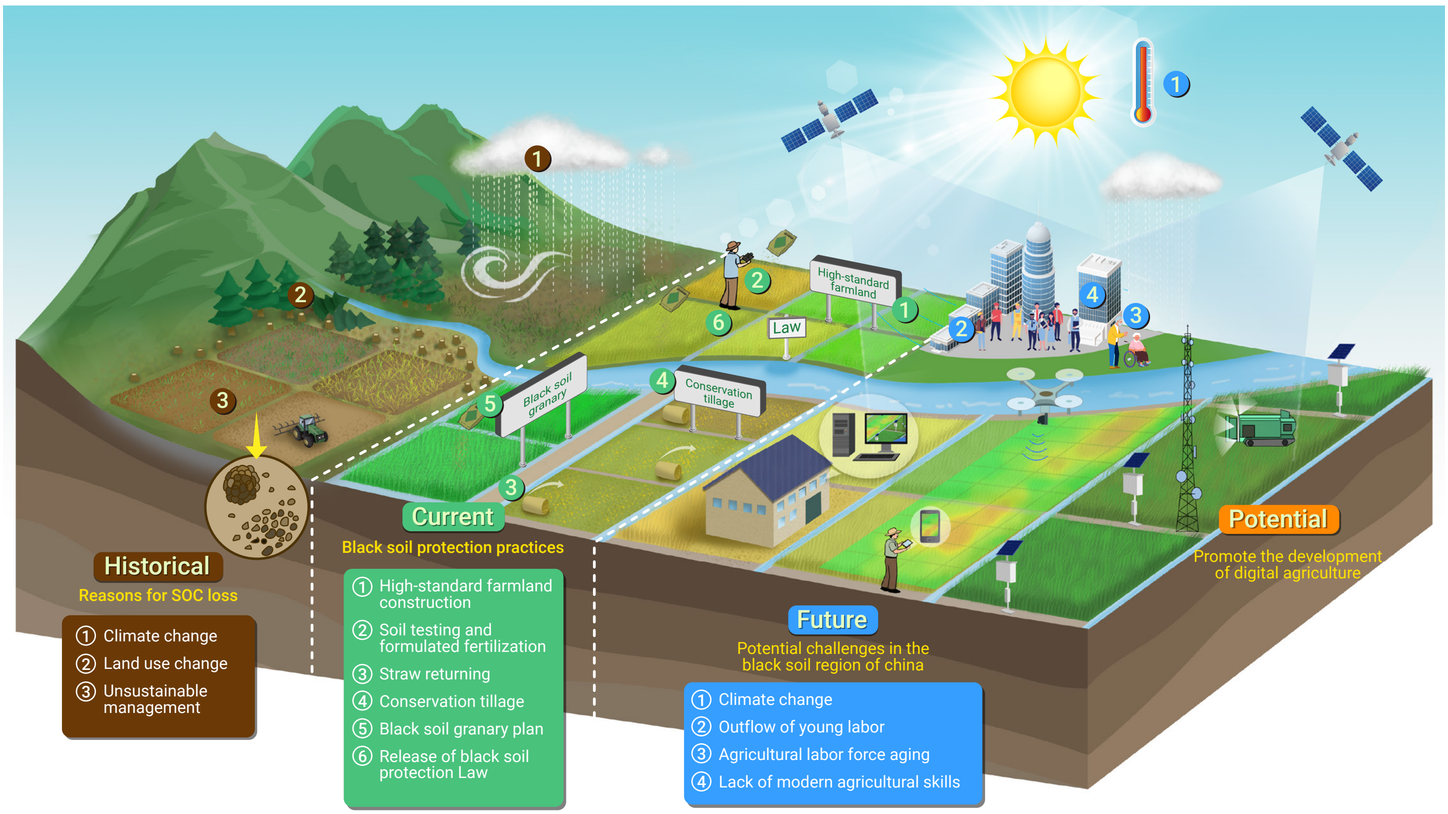

PUBLIC SUMMARY

- Mean soil organic carbon (SOC) in China's black soil region declined by 16.53% over the past four decades.
- Historically, the loss of SOC did not directly exert a strong negative impact on crop yields.
- Under future climate scenarios, topsoil SOC may decline 22%–29% by 2100, threatening long-term food security.
- Digital agriculture is a potential pathway to support the sustainable use of black soils in the future.

Organic carbon loss from the black soil region threatens food security in China

Jian Chen,[1,2,8] Wenyou Hu,[1,2,8,*] Xianghua Xu,[3] Yuxin Tong,[4] Guojing Yan,[1,2] Dongsheng Yu,[1,2] Yuguo Zhao,[1,2] Lixia Ma,[1,2] Enze Xie,[1,2] Yu Zhang,[1,2] Tingrun Zou,[1,2] Zhongjun Jia,[5] Michael L. Thompson,[6] Miguel Angel Taboada,[7] and Yongcun Zhao[1,2,*]
[1]State Key Laboratory of Soil and Sustainable Agriculture, Institute of Soil Science, Chinese Academy of Sciences, Nanjing 211135, China
[2]University of Chinese Academy of Sciences, Beijing 101408, China
[3]School of Ecology and Applied Meteorology, Nanjing University of Information Science and Technology, Nanjing 210044, China
[4]Global Soil Partnership, Land and Water Division, Food and Agriculture Organization of the United Nations, Rome 00100, Italy
[5]Northeast Institute of Geography and Agroecology, Chinese Academy of Sciences, Changchun 130102, China
[6]Agronomy Department, Iowa State University, Ames 50011, USA
[7]College of Agriculture, University of Buenos Aires, Buenos Aires C1417DSE, Argentina
[8]These authors contributed equally
*Correspondence: yczhao@issas.ac.cn (Y.C.); wyhu@issas.ac.cn (W.H.)

Received: September 15, 2025; Accepted: March 10, 2026; Published Online: March 16, 2026; https://doi.org/10.59717/j.xinn-geo.2026.100213

Citation: Chen J., Hu W., Xu X., et al. (2026). Organic carbon loss from the black soil region threatens food security in China. *The Innovation Geoscience* **4**:100213.

Changes in soil organic carbon (SOC) within the world's most fertile black soils pose a major challenge to soil carbon-based climate change mitigation and food security. Yet limited understanding of the spatiotemporal dynamics of SOC across different depths in black soils and their effects on crop yields has constrained sustainable soil management (SSM). Using 18,314 field observations from China's black soil region, we integrated process-based and machine learning approaches to reconstruct and project spatiotemporally consistent SOC time series at the centennial scale. Results show that cropland topsoil (0–30 cm) SOC concentrations decreased from 24.2 to 20.2 g kg^{-1} between 1980 and 2023, with minimal changes in deeper soils. Under future climate scenarios, topsoil SOC may decline by 22%–29% by 2100, potentially reducing crop yields by 263–412 kg ha^{-1}, which corresponds to 5.7%–8.9% of total crop production in Northeast China in 2023. Promoting SSM through digital agriculture could help mitigate declines in SOC and crop yields in China, while global coordination is urgently needed to establish standardized SOC monitoring systems and safeguard the sustainable productivity of black soils worldwide.

INTRODUCTION

Black soils, characterized by a thick (≥ 25 cm), black surface horizon enriched with soil organic carbon (SOC) (Figure 1), play an irreplaceable role in sustainable food production under the changing climate.[1–3] Black soils contain moderate to high SOC concentrations (≥ 1.2%), and are mainly distributed in Eurasia, North America, and South America (Figure S1 & Texts S1-S2).[3,4] Occupying only ~5.6% of global land, black soils nevertheless contribute nearly 10% to total SOC sequestration potential, a proportion markedly greater than that of other mineral soils.[5,6] Crucially, these SOC-rich black soils substantially support agricultural productivity, feeding not only 223 million indigenous people but also supplying a range of commodities to global markets, thereby contributing to global economic development.[5] Therefore, the sustainable management and utilization of SOC in black soils is fundamental to food security and climate mitigation, while also supporting the attainment of multiple United Nations Sustainable Development Goals (SDGs), including SDG 1 (No Poverty) and SDG 2 (Zero Hunger).[7,8]

Of all countries, China contains the world's third-largest black soil area, estimated at ~50 Mha and largely distributed across Northeast China.[9,10] Black soils in China account for only about 9.40% of the nation's arable land, yet they have contributed approximately 20% of national crop production since 2010, exceeding 30% of total crop production in Europe and about 5% globally (Figure 1). As a developing nation with a population exceeding 1.4 billion, China relies on its black soil region as the most important food basket.[11,12] However, global economic and geopolitical crises, together with more frequent occurrences of extreme weather events, have placed increasing pressure on global food production and trade.[13–16] For China, one of the world's largest food importers, these challenges underscore the urgent need to enhance food self-sufficiency, particularly by increasing crop yields through sustainable management practices while ensuring soil health in major crop-producing regions,[16] such as the black soil region. Such efforts not only promote the transition of China's agri-environmental systems toward a sustainable path, but also minimize competition with other developing countries for imported grain, thereby making a significant contribution to the achievement of global SDGs.[17]

Over the past forty years, crop productivity in China's most fertile black soil region has increased steadily (Figure 1), with SOC serving as the cornerstone of soil fertility that sustains these productivity gains.[18–21] However, numerous studies have examined changes in SOC in China's black soils and found that most of these soils have significantly lost SOC, primarily driven by the conversion of natural ecosystems to cropland, unsustainable farming practices (e.g., intensive cultivation), and climate change (e.g., warming).[22–27] Unfortunately, the spatiotemporally consistent long-term time series of SOC for different depths of black soils are still lacking, due to the scarcity of multi-period sample data and model limitations (Text S4). This, in turn, constrains the identification of spatiotemporal patterns of SOC change in black soils, the factors driving these changes, and the design of sustainable soil management strategies. Moreover, previous field experiments have demonstrated that when the SOC level falls below a critical threshold, even a minor loss of SOC can result in a drastic decline in crop yield.[21,28] Yet, at the regional scale, the contribution of long-term SOC dynamics to supporting the high crop yields in China's black soil region remains unclear, particularly under future climate change uncertainty.[29,30] This information is critical for optimizing the use of China's black soils, improving the capacity of croplands to withstand external pressures, contributing to food security, and supporting strategies for climate change mitigation.

To fill this knowledge gap, we collected 18,314 cropland SOC data points across multiple historical periods in Northeast China (Figure S1), and then developed a four-dimensional (4D) (i.e., 3D space plus time) predictive model (RothC-AutoML$_{st}$) that integrates the process-based SOC model and automatic machine learning to reconstruct the spatiotemporal dynamics of SOC across different soil depth intervals from 1980 to 2023. We investigated the drivers of SOC dynamics in croplands of Northeast China, identified the SOC critical thresholds affecting yields of major crops in the region, projected changes in SOC and associated crop yields under future climate conditions, and discussed their implications for promoting the sustainable utilization of black soils to ensure food security in China.

MATERIALS AND METHODS

SOC data and covariates

Our study focuses on croplands of Northeast China (Text S1 & Figure S1), a ~1.47 million km^2 region that encompasses the black soils colloquially known as the "giant pandas in Chinese farmlands". To quantify spatiotemporal changes in cropland SOC during the period 1980–2023, we collected 18,314 SOC samples across six sampling years (Text S3). The SOC concentration in the soil samples was measured using the potassium dichromate oxidation method (external heating)[31]. A range of soil, topographic, climatic, vegetative, and management-related covariates (Table S1) was used to represent envi-

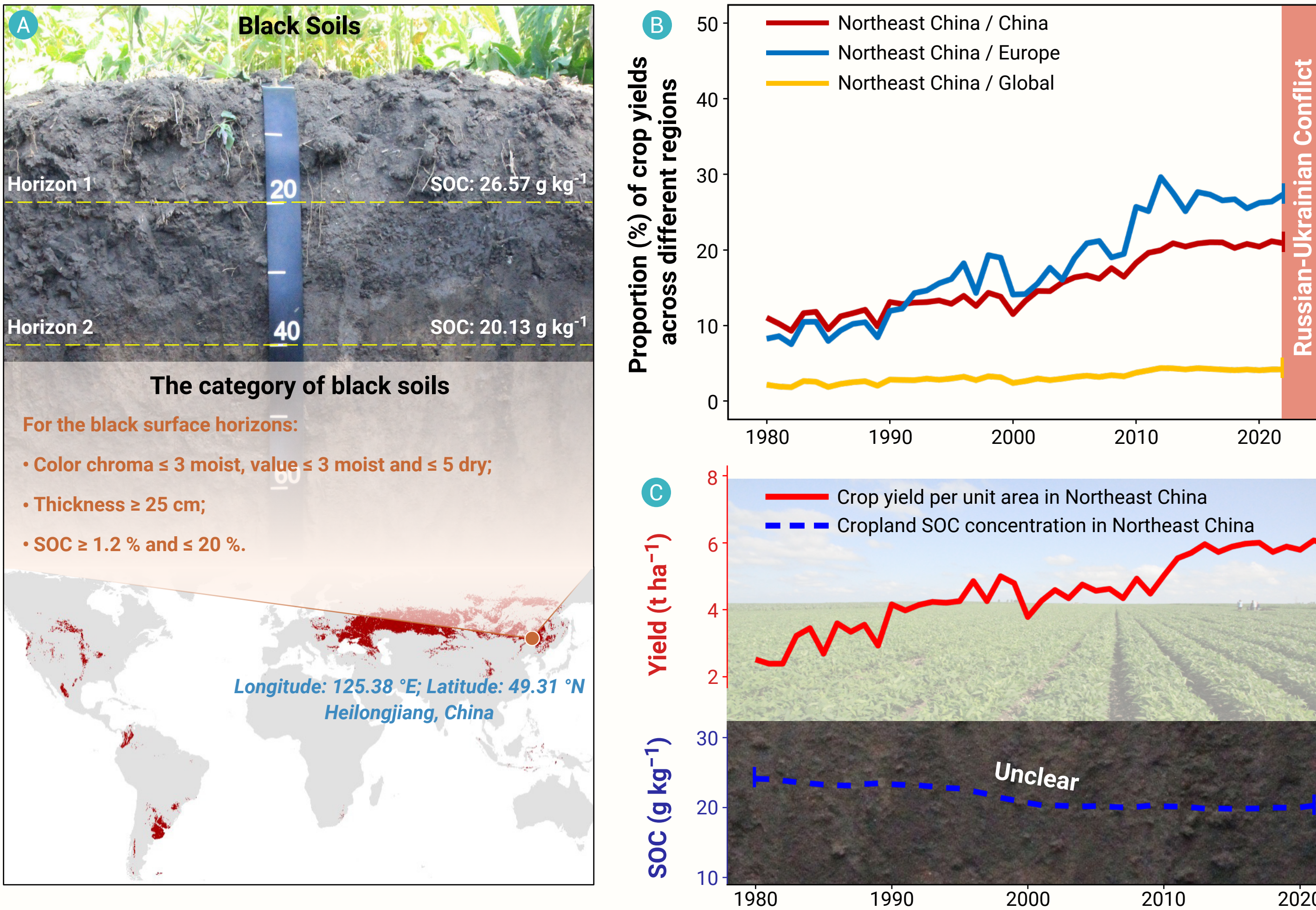

Figure 1. Distribution and soil horizon properties of black soils worldwide, the proportion of crop yields in Northeast China relative to Europe and the world, and crop yields per hectare in Northeast China The profile of black soil in (A) was excavated from Heilongjiang Province (125.38°E, 49.31°N) in Northeast China. Black soils are classified according to the second category defined by the Food and Agriculture Organization of the United Nations (FAO). SOC represents soil organic carbon concentration. Data on crop yields in Europe and across the globe are sourced from the FAO (https://www.fao.org/faostat/en/), and crop yields in Northeast China are obtained from the China Statistical Yearbook (http://www.stats.gov.cn/english/).

ronmental factors driving the spatiotemporal patterns of SOC. The environmental covariates were categorized into two types, that is, static and dynamic.[32,33] The static covariates, assumed to be unchanged over time in this study, included soil classes, soil texture, landforms, lithology, topographic properties, and upper and lower depths of each sampled horizon (Table S1). The dynamic covariates, assumed to change over time, were those related to climate, vegetation, land use, and management (Table S1). To overcome the shortcomings of space-for-time substitution (Text S4), the SOC simulated by the process-based RothC model was also used as a dynamic covariate in machine learning modeling.[34,35]

Four-dimensional dynamic modeling of SOC

Following the SCORPAN framework for digital soil mapping,[36–38] we developed an integrated model (RothC-AutoML$_{st}$) combining the process-based model (RothC), automatic machine learning (AutoML), and space-for-time substitution for reconstructing SOC dynamics across multiple soil depths during 1980–2023 (Text S4). The development of the RothC-AutoML$_{st}$ model includes four steps: SOC baseline modeling, RothC simulation, model integration, and accuracy evaluation. Details for each step are shown in Text S4. Twenty percent of the samples were held out for independent validation, and the evaluation indicated that RothC-AutoML$_{st}$ accounted for 67% of the variation in the SOC validation data, with Lin's concordance correlation coefficient of 0.78 and mean absolute error of 7.87 g kg^{-1} (Figure S2). Regarding different soil depths, the RothC-AutoML$_{st}$ model explained 79% of SOC variation at 0–30 cm, 76% at 30–60 cm, and 46% at 60–100 cm (Figure S2).

Using the annual SOC grids (1980–2023) at 500 m resolution generated by RothC-AutoML$_{st}$, we computed regional SOC time series for both the entire study area and individual counties by averaging the grid values. This approach allowed us to examine temporal patterns in SOC changes. To estimate the rate of SOC change at the grid-cell level, linear regression analysis was conducted for each grid cell, as described by the following equation:

$$SOC(i) = \beta_0(i) + \beta_1(i) \cdot Year_i + \varepsilon(i), \quad (1)$$

where *SOC(i)* is the predicted cropland SOC level (g kg^{-1}) at grid cell *i* for a given year; *Year* is the corresponding year; β_0 is the intercept; ε is the residual error; β_1 is the regression slope, representing the rate of cropland SOC change (g kg^{-1} yr^{-1}). Spatial uncertainty in the estimated change rate of SOC was characterized by the 2.5th and 97.5th percentiles of the regression slope's confidence interval. We applied a random forest model to quantify the influence of environmental covariates on topsoil SOC change rates, with further details provided in Text S5.

Future projection of SOC

As a mid- to high-latitude region, Northeast China has experienced pronounced climate change over the past century, with a mean annual temperature increase of 0.16°C per decade. Therefore, to examine projected climate-driven changes in long-term SOC dynamics, we re-ran RothC and further retrained the RothC-AutoML$_{st}$ model based on future climate data and projected net primary production (NPP) data. We assumed that future human management practices remain unchanged and that SOC dynamics are mainly driven by future climate and corresponding NPP dynamics. Three future dynamic variables (precipitation, temperature, and potential evapotranspiration) from January 2024 to December 2100 were obtained from a publicly available dataset released by the Chinese Academy of Sciences.[39] Three Shared Socioeconomic Pathway (SSP) scenarios were considered in this study: SSP1–1.9 (low radiative forcing), SSP2–4.5 (intermediate radiative forcing), and SSP5–8.5 (high radiative forcing).[40] The corresponding NPP for the three SSP scenarios from 2024 to 2100 was primarily obtained using the space-for-time AutoML ($AutoML_{st}$). Briefly, relationships between historical NPP and climate factors (mean annual precipitation, temperature, and potential evapotranspiration), along with a series of static covariates (mainly soil and terrain factors), were established using $AutoML_{st}$. Climate variables under different scenarios were subsequently fed into the trained $AutoML_{st}$ model to project future NPP. Validation results of $AutoML_{st}$ showed that the model explained 94% of the NPP variation. The *RMSE* and *MAE* were 38.18 g C m^{-2} and 27.42 g C m^{-2}, respectively, indicating that the $AutoML_{st}$ model accurately simulated NPP. The spatiotemporal patterns of SOC at 0–30, 30–60, and 60–100 cm depths over the period of 2024–2100 under three climate scenarios are shown in Supplementary Videos 4–12.

Detection of critical threshold of SOC for crop yields

Here, partial least squares path modeling (PLS-PM) was applied using the R package *plspm* to assess the effects of SOC and environmental factors on the yields of three major crops in Northeast China. Yield data for rice, maize, and soybean were sourced from Iizumi and Sakai (2020).[41] We first resampled annual SOC and environmental factor maps to ensure consistency with the crop yield data resolution. Outliers were then removed based on the mean ± three standard deviations (SD) criterion, resulting in a final yield dataset of 14,039 observations during the period 1981–2016. This dataset was used to construct the data matrix for both the PLS-PM analysis and the threshold regression. To quantify the independent contribution of SOC to crop yields, we controlled for the effects of fertilization, mean annual temperature, aridity index, radiation flux, and spatial position (latitude and longitude). To account for temporal autocorrelation, year was modeled as a first-order autoregressive structure. To detect critical SOC thresholds, we followed a method adapted from Berdugo et al. (2022)[42]. That is, both linear and nonlinear (generalized additive model, GAM) regressions were fitted between crop yield and SOC while accounting for the above controlling factors. A SOC threshold was considered to exist only when the nonlinear model had a lower Akaike Information Criterion (AIC) than the linear model.[43] Once a threshold was identified, it was quantitatively estimated using a two-phase segmented regression of the form:[44]

$$\eta = \varepsilon + a_2^T z + \beta_1 (x - e)_+ + \beta_2 x, \tag{2}$$

where *e* represents the critical SOC threshold; *x* represents the SOC subject to a threshold effect, and *z* denotes other control variables. The hinge term $(x\text{-}e)_+$ equals *x-e* when *x* exceeds *e* and otherwise equals zero. Coefficients β_1 and β_2 correspond to the slopes of the two linear segments. ε is the residual. The uncertainty of the estimated threshold was quantified using a nonparametric bootstrap procedure with 1000 resamples. In each bootstrap iteration, observations were resampled with replacement from the original dataset, and the full threshold regression model was refitted. The standard error (SE) of the threshold was derived from the standard deviation of bootstrap estimates, providing an empirical measure of its sampling variability and uncertainty. Because mean annual precipitation and temperature were highly collinear, mean annual precipitation was excluded from the model to avoid inflated parameter estimation errors. The *gam* package in R was used to fit GAM and the *chngpt* package was used to fit two-phase segmented regressions.

RESULTS AND DISCUSSION

Annual dynamics of SOC

The results of RothC-$AutoML_{st}$ showed that the modeled mean topsoil (0–30 cm) SOC concentration in all croplands of Northeast China decreased significantly from 24.2 g kg^{-1} in 1980 to 20.2 g kg^{-1} in 2023, representing an average loss rate of 0.11 (95% confidence interval [CI]: 0.10–0.13) g kg^{-1} yr^{-1} (Figure 2A). Overall, the topsoil SOC loss was severe before 2001, but tended to slow down thereafter (Figure 2A). For croplands with relatively high initial SOC concentration (> 75% quantile of SOC concentration in 1980), the average topsoil SOC loss (-7.6 g kg^{-1}) was relatively severe, with a high loss rate of 0.17 (95% CI: 0.14–0.20) g kg^{-1} yr^{-1}. In contrast, for croplands in Northeast China with relatively low initial SOC concentration (< 25% quantile of SOC concentration in 1980), the SOC in topsoil tended to increase slightly (0.4 g kg^{-1} over 43 years), with an average accumulation rate of 0.02 (95% CI: 0.01–0.02) g kg^{-1} yr^{-1} (Figure 2A). These results suggested that the levels of initial SOC significantly affected the trend of topsoil SOC change.[45] For the 30–60 and 60–100 cm soil layers, the average decrease in SOC over the period of 1980–2023 was minimal (Figures 2B-C).

For croplands within Northeast China's typical black soil region (a subset of regional soils) (Figure S1), the modeled average loss of topsoil SOC was severe (-3.6 g kg^{-1}), with an average loss rate of 0.12 (95% CI: 0.10–0.13) g kg^{-1} yr^{-1} (Figure 2D). At depths of 30–60 and 60–100 cm in the black soil region (Figures 2E-F), the levels of SOC concentration remained relatively stable over the period of 1980–2023. It should be noted that, compared to the in-situ monitored SOC concentration from different field sites, the SOC predicted by RothC-$AutoML_{st}$ showed some minor numerical discrepancies (Figure S3). Yet, their interannual variation trends were closely consistent, suggesting that the reconstructed spatiotemporal dynamics of SOC are highly reliable.

Spatial patterns of SOC change

The spatial patterns of topsoil SOC change in croplands of Northeast China are presented in Figure 3. Overall, the soils in the northern and northeastern parts of the study area tended to lose SOC over the 43-year period, while those in the southern parts accumulated SOC (Figure 3A). Heilongjiang Province presented a significant decline in topsoil SOC over that period (Figure 3A). For example, the average rates of SOC loss in croplands of Hulin County and Baoqing County of Heilongjiang Province were approximately 0.6 g kg^{-1} yr^{-1} and 0.5 g kg^{-1} yr^{-1}, respectively (Figure 3B). In Jilin Province, the loss of SOC mainly occurred in the southeastern parts of the province (Figure 3A), while the northwestern parts tended to accumulate SOC. For example, the SOC accumulation rate of Shuangliao County was highest in the province, averaging 0.05 g kg^{-1} yr^{-1} (Figure 3C). In addition, most of the croplands in Liaoning Province accumulated SOC over the period 1980–2023, except for the coastal areas (Figure 3A). Overall, the change rate of topsoil SOC in croplands exhibited relatively low uncertainty (Figure S4).

From 1980 to 2023, about 21.9 Mha of cropland exhibited significant (P < 0.05) topsoil SOC loss, representing roughly 61% of Northeast China's cropland area (Figure 3D). Areas with significant topsoil SOC accumulation reached 7.6 Mha (~21%), while the topsoil SOC changes for ~18% of the croplands were not significant (Figure 3D). Besides, the areas where SOC declined over the period 2000–2023 were reduced, compared to those over the period 1980–2000, indicating that the cropland topsoil SOC loss in most parts of Northeast China slowed down during the recent two decades (Figure S5). At 30–60 and 60–100 cm, estimated SOC changes across croplands in Northeast China were slight, whereas uncertainties were substantially larger than those for topsoil (Figures S4-S6).

Driving factors of the SOC change

The variable importance analysis showed that initial SOC level in 1980 was the most important covariate in affecting the rate of topsoil SOC change, accounting for the highest relative importance of 53.63% in explaining the variations of SOC change rate (Figures 4A-B). Soils with high initial SOC tended to lose soil carbon after cultivation. Such a negative baseline effect has been widely observed in the SOC-rich black soils, for example, the black soils in Ukraine,[46] the United States,[47] and Argentina.[48] Covariates representing climate, soil properties, and management practices are also quite important (Figure 4), as they largely govern SOC dynamics at regional scales.[49–52] Within soil properties, soil pH showed a high relative importance, reflecting its integrative control on SOC turnover by regulating microbial community structure, enzyme activity, and organic matter decomposition rates.[3] Moreover, spatial variations in pH at the regional scale reflect long-term pedogenic processes and anthropogenic influences, thereby enhancing its explanatory power for SOC change.

In addition, the contribution of years in cultivation to SOC loss should not be overlooked, even though its relative importance was less than that of the

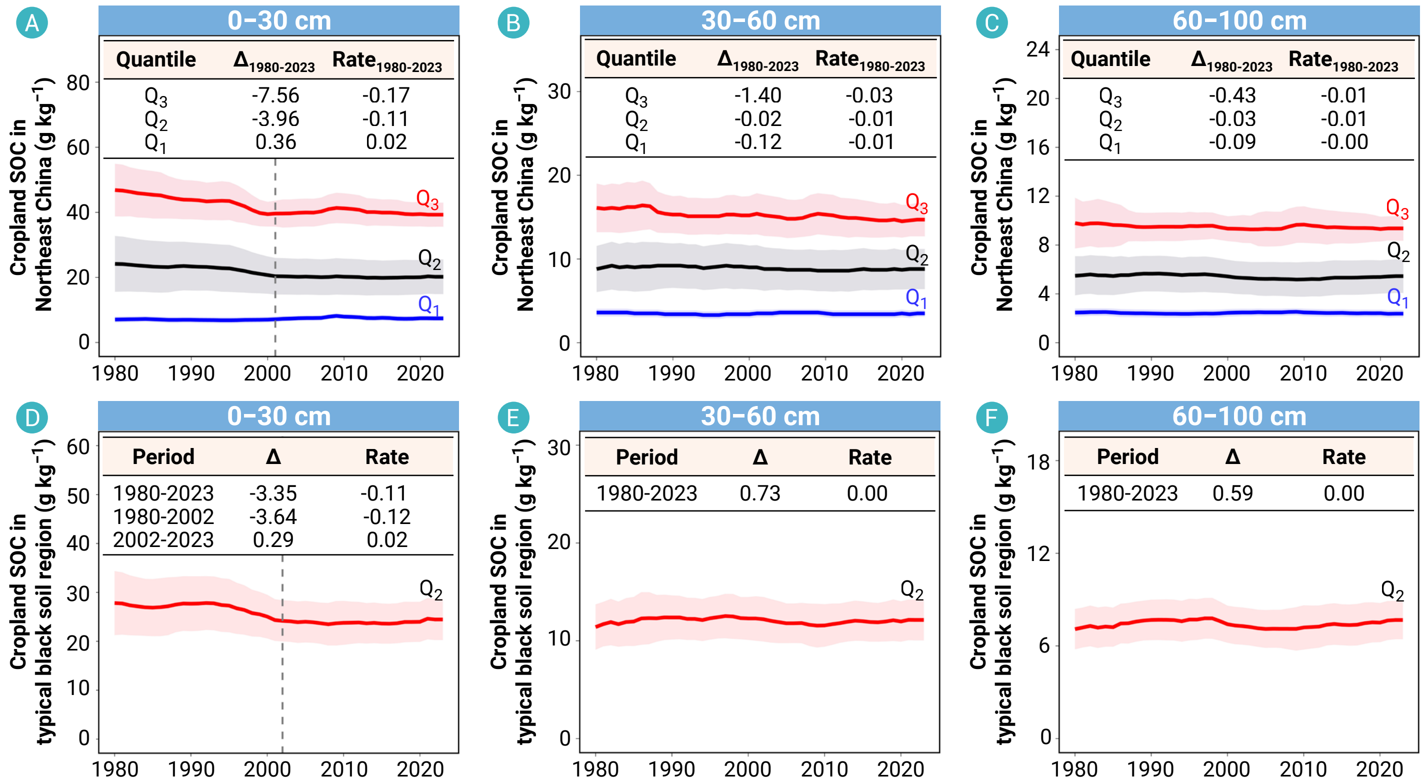

Figure 2. Time series of cropland soil organic carbon (SOC) concentration for different soil depth intervals in Northeast China and its typical black soil region The red and blue solid lines in (A–C) represent the mean SOC concentration in the high-carbon (Q_3) and low-carbon (Q_1) regions, respectively. High carbon is defined as SOC concentration being greater than 75th quantile of the SOC values in 1980. Low carbon is defined as SOC concentration being less than 25th quantile of the SOC values in 1980. The black solid line in (A–C) and red solid line in (D–F) represent the mean SOC concentration (Q_2). The shading in (A–F) denotes 50% of the standard deviation of modeled predictions for all grid cells for each year. Δ represents change in SOC concentration (g kg^{-1}). Rate represents SOC change rate (g kg^{-1} yr^{-1}), derived from a linear regression of the annual mean SOC concentration and year.

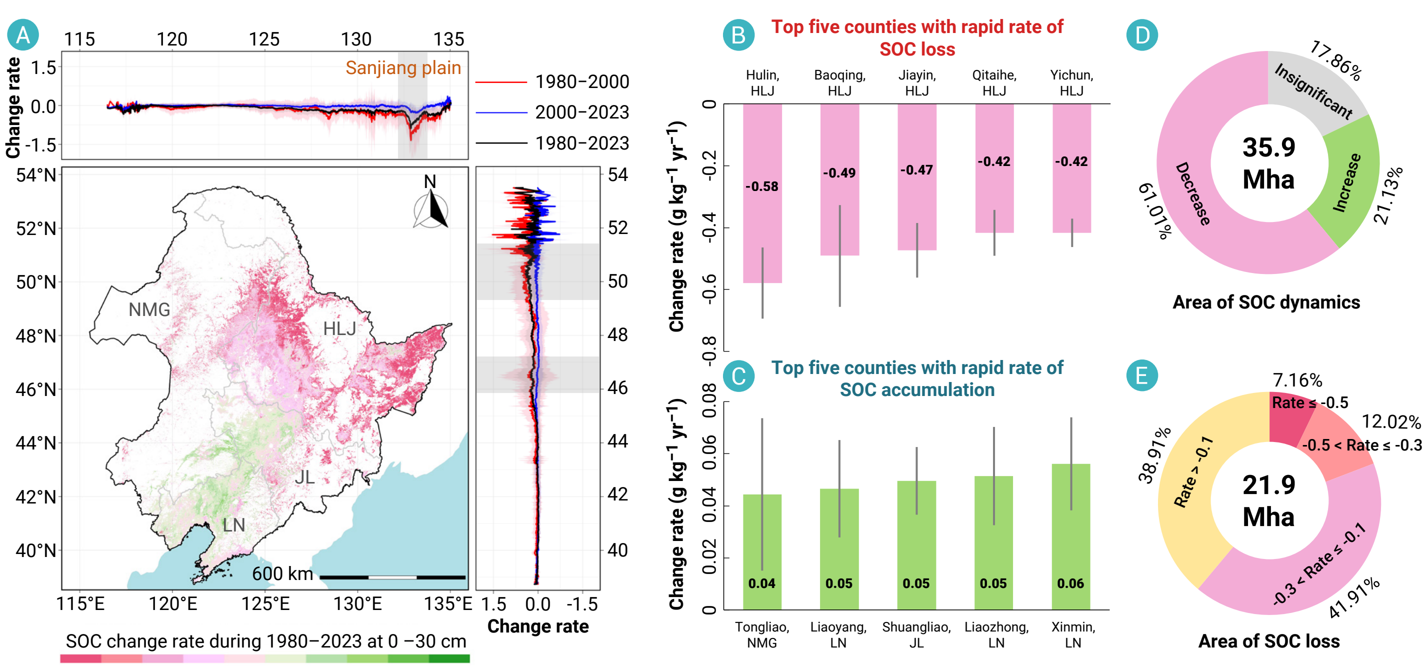

Figure 3. The spatial patterns, county-level statistics, and area of cropland soil organic carbon (SOC) change at 0–30 cm in Northeast China, 1980–2023 Error bars in (B–C) indicate the standard deviation of SOC change rate in cropland grid cells within the corresponding counties. Spatiotemporal dynamics of cropland SOC concentration at 0–30, 30–60, and 60–100 cm depths over the period of 1980–2023 are shown in Supplementary Videos S1–S3, respectively.

other twelve important covariates (Figure 4A). On average, a turning point in topsoil SOC dynamics occurred after 23 years of cultivation in Northeast China's croplands. (Figure 4C). Specifically, the average SOC concentration at 0–30 cm decreased rapidly during the first 23 years of cultivation, and although continuous cultivation followed, the rate of SOC loss gradually slowed. The overall regional-scale trend of SOC change in croplands of Northeast China was consistent with that identified by the long-term field experiments on black soils. For example, changes in SOC in black soils typically

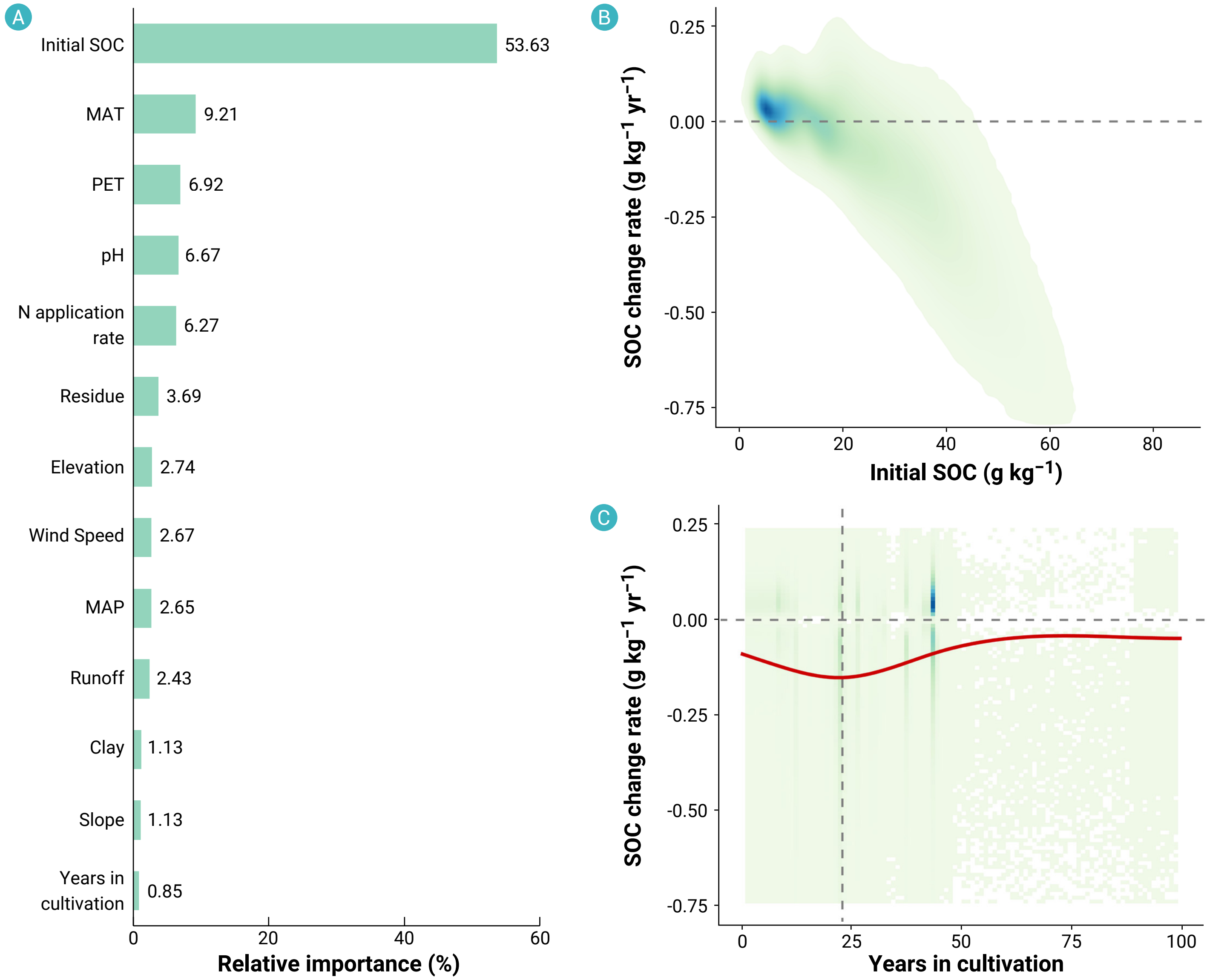

Figure 4. Key drivers of changes in topsoil (0–30 cm) soil organic carbon (SOC) across Northeast China's croplands (A) Relative importance of covariates for predicting topsoil SOC change; (B) linear regression of SOC change rate on initial SOC level; and (C) non-linear regression of SOC change rate on years in cultivation. Full details of the data and methods for driver analysis are provided in Text S5. Variable full names are listed in Table S1.

exhibited two distinct phases, closely associated with the transition from natural to cultivated soils.[11] The first stage is characterized by a rapid SOC decline during the first ~30 years after cultivation, mainly due to land conversion from natural vegetation to crops, reduced carbon input following harvest of above-ground biomass, and increased soil disturbance and gas exchange from tillage. The second stage is represented by the steady decrease in loss rate of SOC, primarily due to increased organic matter from crop residue return, fertilizer application, and adoption of conservation tillage.

Critical threshold of SOC for maintaining crop yields

Using major crop yields and various environmental factors, PLS-PM confirmed that climate change negatively affected crop yields, while fertilization and SOC positively affected yields in the fertile croplands of Northeast China (Figure 5A). Indeed, an increase in SOC has been widely shown to enhance crop yields by increasing water and nutrient availability, promoting soil structural quality, and supporting soil biotic functions,[18] even in regions with relatively high indigenous soil fertility. For example, previous studies have found that a 1-ton increase in SOC stock led to wheat yields increasing by 27 kg ha^{-1} in the North American Great Plains[53] and 40 kg ha^{-1} in the Pampas of Argentina,[54] both of which are major black soil regions globally, with relatively high SOC. However, it is crucial to highlight that climate change is also accelerating SOC depletion, endangering the sustainability of future crop yields (Figure 5A).

After statistically controlling for fertilization, climate, and crop types, increasing SOC positively influenced major crop yields, while the SOC-yield relationship remained nonlinear (Table S2). A tipping point exists in the SOC concentration where crop yield declined rapidly with decreasing SOC, but increased slowly with increasing SOC (Figure 5). Such a tipping point is recognized as a critical threshold of SOC for maintaining crop yield,[21] that is, the SOC level that may significantly constrain the crop yield once being lower than this threshold. On average, the critical threshold of SOC for the entire croplands of Northeast China was about 18.0 g kg^{-1}, with a SE of 0.6 g kg^{-1} (Figure 5B & Table S3). A SOC decrement of 1 g kg^{-1} may cause a crop yield decline of ~150 kg ha^{-1} when SOC in the topsoil of Northeast China falls below this critical threshold (Figure 5B). For all croplands of Northeast China, the modeled average topsoil SOC concentrations in 1980 and 2023 were 24.2 g kg^{-1} and 20.2 g kg^{-1}, respectively, exceeding the estimated critical threshold (18.0 g kg^{-1}). This implies that, although average SOC declined over the 43-year period, SOC levels did not substantially reduce mean crop yields in the region (Figure 5B).

Additionally, the estimated SOC thresholds for the three major crops in Northeast China were quite similar, namely 18.9 g kg^{-1} (SE = 0.2 g kg^{-1}) for

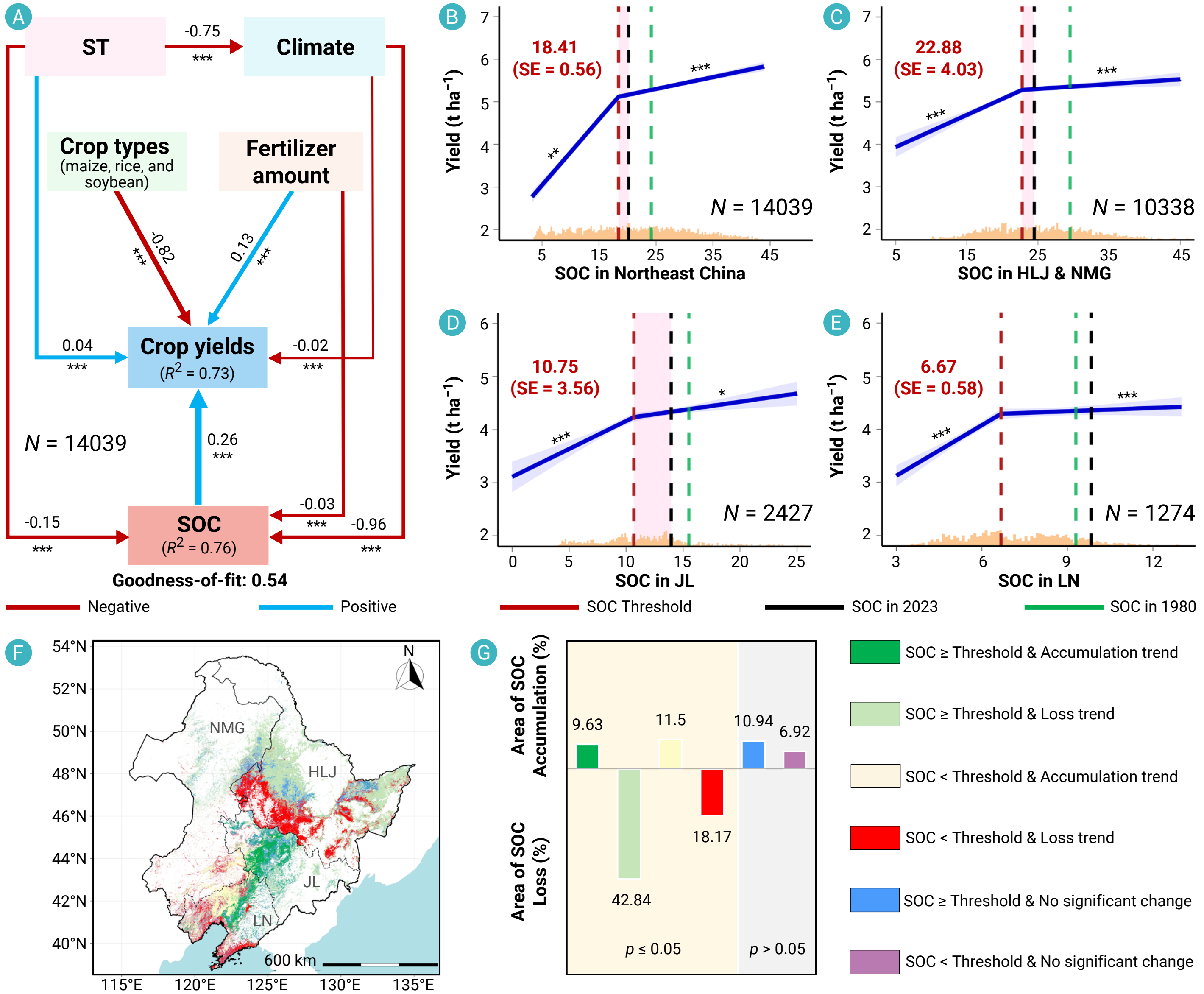

Figure 5. Relationships between soil organic carbon (SOC) at 0–30 cm and crop yield (A) Partial least squares path model of the effects of SOC and environmental factors on crop yields: negative and positive effects are depicted by red and blue arrows, with standardized path coefficients displayed on the paths; ST represents space-time variables (longitude, latitude, and year). (B–E) Nonlinear relationships between SOC and crop yields; the light blue shaded areas are 95% confidence intervals; the red dashed line represents the SOC critical threshold; histogram (orange bars) in (B–E) represent the value distribution of SOC concentration; HLJ, NMG, JL, and LN represent Heilongjiang, Inner Mongolia, Jilin, and Liaoning Province, respectively. *N* represents number of samples; Asterisks denote statistical significance: * $P < 0.05$, ** $P < 0.01$, *** $P < 0.001$. (F–G) The spatial distribution characteristics of SOC in 2023 and the associated area proportions, combined with the SOC change rate over the past four decades and the corresponding critical thresholds. The *p* values were derived from a cell-by-cell linear regression of the SOC and year.

maize, 17.8 g kg^{-1} (SE = 0.3 g kg^{-1}) for rice, and 18.8 g kg^{-1} (SE = 0.3 g kg^{-1}) for soybeans (Tables S4-S5 & Figure S7). However, regional differences in the identified SOC critical thresholds among the provinces were also evident. The average SOC critical threshold for croplands was highest in Heilongjiang and Inner Mongolia at 22.9 g kg^{-1} (SE = 4.0 g kg^{-1}), lowest in Liaoning at 6.7 g kg^{-1} (SE = 0.6 g kg^{-1}), and intermediate in Jilin at 10.8 g kg^{-1} (SE = 3.6 g kg^{-1}) (Figures 5C-E). Overall, the average SOC threshold levels for Heilongjiang and Inner Mongolia and Jilin were still higher than their corresponding thresholds, but the range allowed for further loss of the SOC was quite narrow (the light-pink shaded areas in Figures 5B-E). Although 61.01% of the croplands in Northeast China had experienced significant SOC loss over the past four decades (Figure 3D), 42.84% of these croplands still had SOC levels above the critical threshold in 2023 (Figure 5G). These croplands were mainly distributed in northern Northeast China, including much of the Sanjiang Plain and Jilin Province (Figure 5F). Of particular concern are the croplands that experienced significant SOC loss over the past four decades and had SOC levels below the critical threshold in 2023. These areas, representing 18.17% of the total area, were primarily distributed in the southwestern part of Heilongjiang Province and the southern regions of Inner Mongolia (Figures 5F-G). Overall, these findings imply that containing the decline of SOC in croplands of these provinces and subareas is quite urgent.

Climate change-induced SOC loss and its threats to food security

In Northeast China, croplands with relatively high initial SOC levels are particularly susceptible to future climate change, especially under increasing human interventions.[55,56] Here, the spatiotemporal dynamics of SOC in these soils were projected over the period 2024–2100 under SSP 1–1.9, SSP 2–4.5, and SSP 5–8.5. Overall, the spatial distribution patterns of topsoil SOC changes in the croplands of Northeast China under the three scenarios, assuming no changes in future human management measures, were similar (Figure 6). Compared to the reference period (1980–2023), most croplands in Liaoning and western Jilin were predicted to accumulate SOC, whereas croplands in northern and eastern Heilongjiang were expected to lose SOC over the 76-year period, with losses in some areas exceeding 30% (Figure 6).

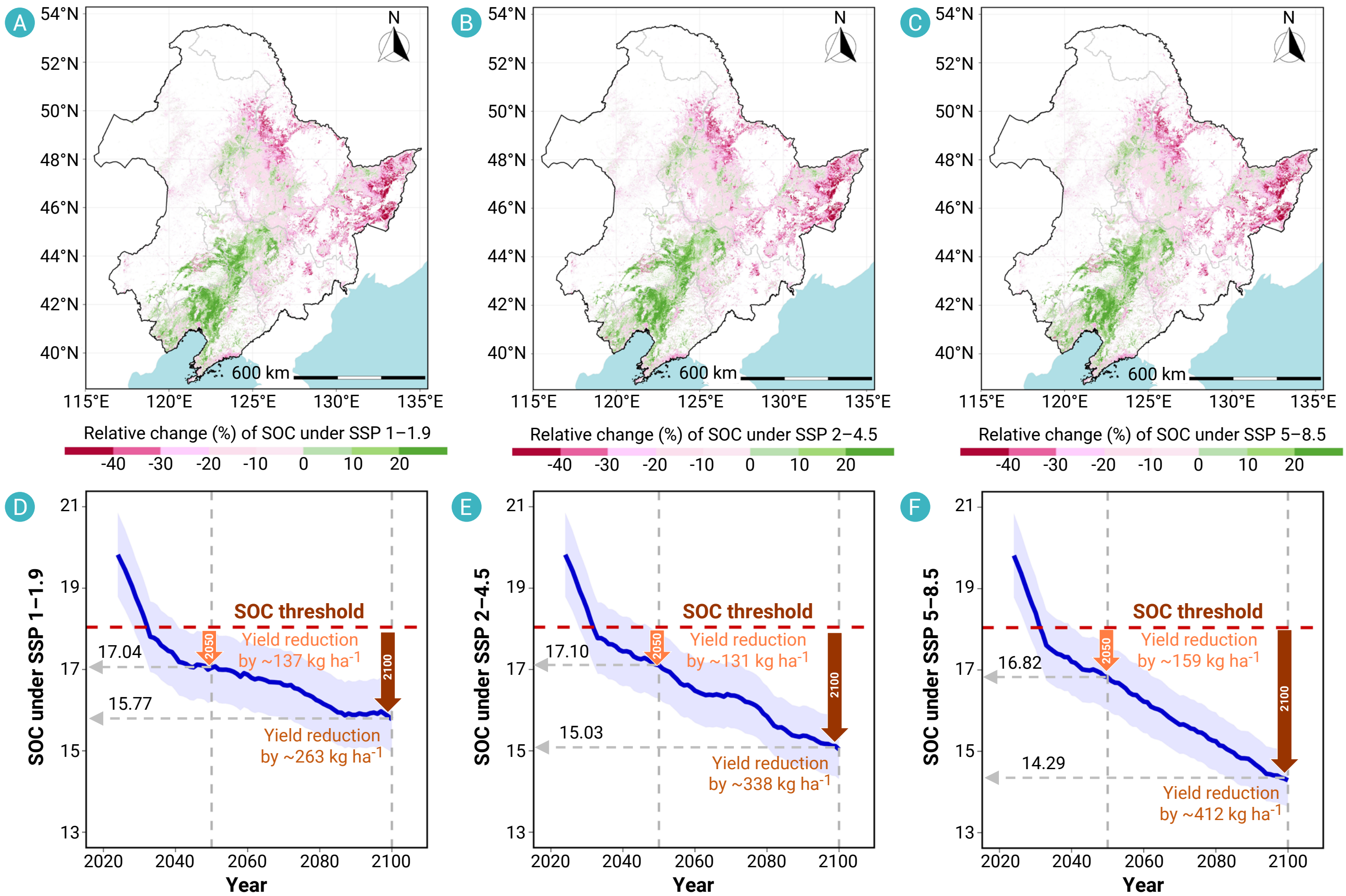

Figure 6. Spatiotemporal changes in cropland soil organic carbon (SOC) (g kg^{-1}) at 0–30 cm and its impact on crop yields under Shared Socioeconomic Pathways (SSPs) scenarios in Northeast China (A–C) Relative change in SOC from 2024 to 2100 under SSP 1–1.9, SSP 2–4.5, and SSP 5–8.5, respectively, with a reference period of 1980–2023. The relative change is calculated as: (mean SOC of the period 2024–2100 - mean SOC of the reference period) / mean of the reference period. (D–F) Time series of SOC and the yield reduction under SSP 1–1.9, SSP 2–4.5, and SSP 5–8.5, respectively. The blue shading denotes 50% of the standard deviation of modeled predictions for all grid cells for each year. The red dashed line represents the SOC critical threshold. Spatiotemporal dynamics of cropland SOC at 0–30, 30–60, and 60–100 cm depths over the period of 2024–2100 under three SSPs are shown in Supplementary Videos 4–12, respectively.

Generally, the topsoil SOC by 2050 is projected to be 17.0 ± 8.2 g kg^{-1} under SSP 1–1.9, 17.1 ± 8.2 g kg^{-1} under SSP 2–4.5, and 16.8 ± 8.0 g kg^{-1} under SSP 5–8.5. By 2100, the loss of topsoil SOC is predicted to be further accelerated under the three SSPs; that is, SOC is predicted to decrease by 22%, 26%, and 29% under SSP 1–1.9, SSP 2–4.5, and SSP 5–8.5, respectively, in comparison with those of 2023. Additionally, the SOC in the deep soil layers (30–60 and 60–100 cm) is projected to decrease under the three scenarios, but the differences in deep-layer SOC decrement among the three scenarios are relatively small (Figure S8).

Overall, future climate-driven SOC losses are expected to bring SOC below the critical threshold of 18.0 g kg^{-1}, thereby decreasing crop yields in Northeast China. Specifically, by 2100, the reductions in crop yields due to SOC loss are projected to be 263 kg ha^{-1} under SSP 1–1.9, 338 kg ha^{-1} under SSP 2–4.5, and 412 kg ha^{-1} under SSP 5–8.5 (Figures 6D-F). Significantly reduced crop yields are predicted mainly to occur in the north and east of Heilongjiang Province where the SOC level may drop below the critical threshold and become a major constraint to soil fertility (Figure 6). Thus, to ensure crop productivity under future climate change in Northeast China, improvement of the SOC levels and basic soil fertility of croplands through sustainable soil management are critically important, especially for the croplands of Heilongjiang Province.

Towards sustainable management of black soils in China for food security

Our results, together with those of Wang et al. (2023)[25] and Meng et al. (2024)[26], show that cropland topsoil SOC declined markedly over the past four decades in Northeast China (Table S6). By incorporating a substantially larger sample size and integrating machine learning with process-based modeling that accounts for SOC turnover, this study provides a more robust and accurate assessment of SOC dynamics across multiple soil depths. Our analysis further shows that average topsoil SOC decreased at a faster rate during 1980–2001 compared with 2002–2023. The change rates of topsoil SOC exhibited significant spatial variation due to intrinsic regional differences (e.g., climate and initial carbon concentration). Fortunately, nearly 40% of the croplands exhibited either a significant increase or no significant change in topsoil SOC concentration. Additionally, our results indicate that SOC decreases in deep soil layers (≥ 30 cm) were minimal, in contrast to the findings of Zhou et al. (2025)[27], which indicates relatively high uncertainty in the spatiotemporal dynamics of SOC in deep soil layers in the black soil region of China. In this study, we compiled soil profile observations spanning a wide spatial and temporal range, and the number of profiles used for modeling was substantially greater than in previous studies. However, compared with topsoil samples, soil profile observations remain relatively limited. This limitation inevitably increases uncertainty in the spatiotemporal changes of SOC in deep soil layers. More importantly, high-resolution dynamic covariates that effectively characterize deep soil environmental conditions are still severely lacking. For example, existing high-resolution remote sensing data cannot directly capture the spatiotemporal variability of environmental conditions in deep soil (e.g., temperature and moisture). Given these constraints, the direction and magnitude of SOC changes in deep soil layers of Northeast China remain uncertain.

The SOC loss across Northeast China still has no significant negative effects on the crop yields. Yet, the influences of SOC levels on crop yield

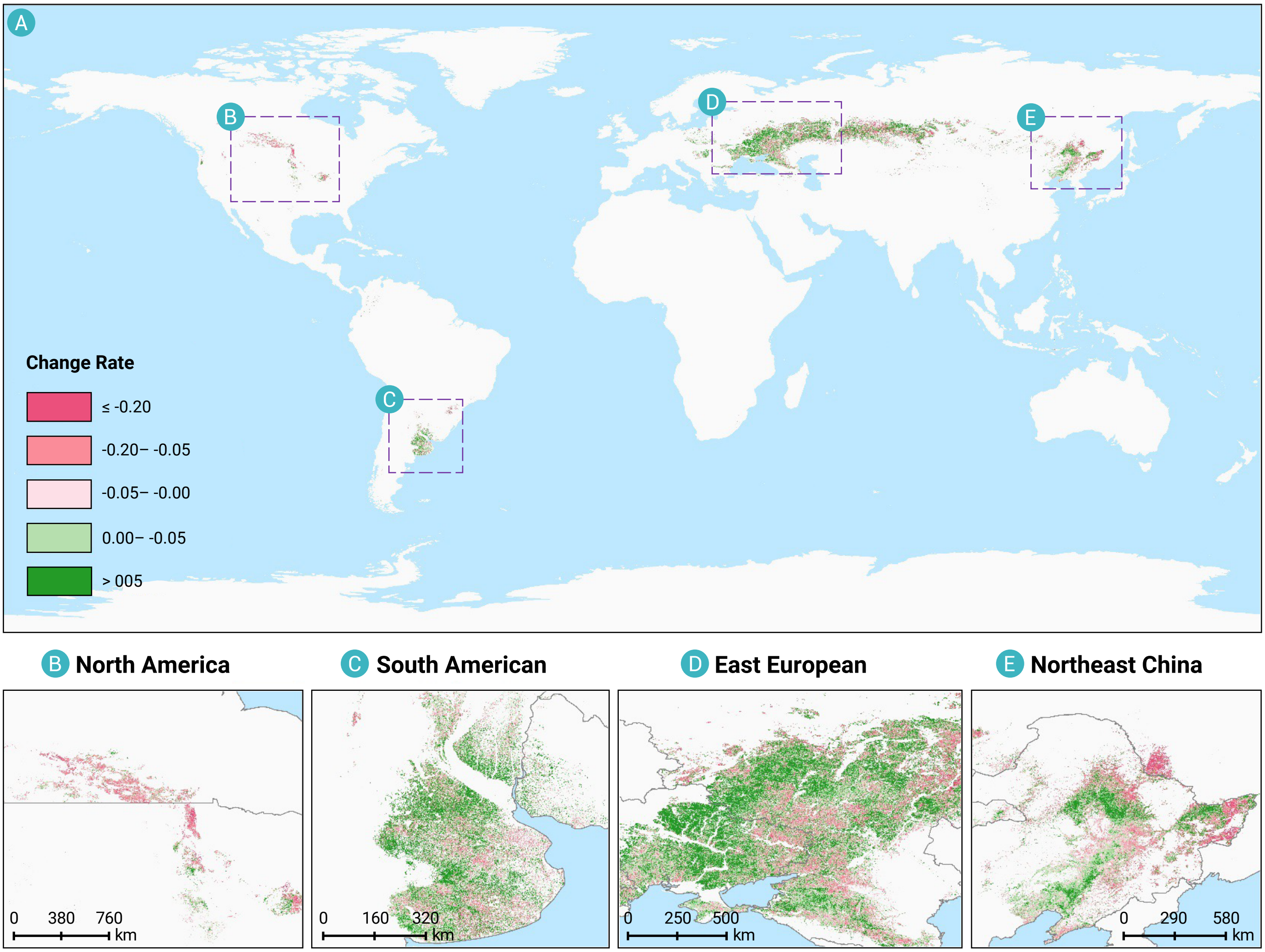

Figure 7. Spatial patterns of change rates (g kg^{-1} yr^{-1}) of cropland soil organic carbon (SOC) at 0–30 cm depth across global black soil regions during 2000–2022 The change rates were derived from a cell-by-cell regression analysis based on SOC values across multiple years. SOC data for different years in the black soil regions of Great Plains of North America (B), Pampas of South America (C), and East European Plain (D) were obtained from https://openlandmap.org/, while those for Northeast China (E) were obtained from this study. Detailed information on global black soil regions and their associated SOC datasets is provided in Text S2.

should not be overlooked, as climate warming may accelerate the SOC decomposition, and cause SOC levels to drop below the critical threshold (18.0 g kg^{-1}), thereby affecting the crop yield. Our estimates indicate that, under the three future climate scenarios, continued SOC loss could lead to yield reductions of 9.47–14.82 million tons for the three major crops in Northeast China by the end of this century. Considering the average per capita grain consumption of China (annual 400 kg per capita)[57], such yield loss accounts for the annual food demand of 23.7–37.0 million people. Northeast China contributes nearly 25% of China's grain production. Although China is broadly self-sufficient in staple grains, its edible oil and animal feed industries are highly dependent on the imported soybeans, while Northeast China is the major soybean production area of China. Consequently, yield reduction resulting from continued SOC loss from Northeast China is not trivial for China, but a direct and huge risk linked to the stability and resilience of the national food security. In addition, China's black soil region is subject to multiple degradation pressures, including soil thinning, compaction, and acidification. These degradation processes, together with the loss of SOC may further lower the soil fertility and amplify the stress on crop production. Therefore, with the rising geopolitical uncertainty and price fluctuation of global food market, achieving sustainable management of black soils in Northeast China has become a critical requirement for safeguarding food security.

The loss of cropland SOC in Northeast China has raised concern among the scientific community and decision-makers.[58,59] Thus, a range of programs and policy measures have been introduced to prevent the SOC loss and enhance crop productivity in Northeast China. These measures include the high-standard farmland construction (characterized by well-leveled, contiguous plots with advanced irrigation), soil testing and formulated fertilization, straw return, black soil granary plan, and the release of Black Soil Protection Law of the People's Republic of China.[12] Within this comprehensive policy framework, conservation tillage practices are particularly important for preventing black soil degradation from the intensive land use in Northeast China. For example, the Lishu-Mode[58] of black soil conservation, which integrates no- or reduced-tillage with straw mulching and optimized crop management, has been successfully promoted and applied in Jilin Province of Northeast China, and the Longjiang-Mode[58] in Heilongjiang Province of China as well. These soil use and conservation modes may offer valuable experiences and lessons for other countries with abundant black soil resources. Considering the economic costs and benefits, the government should prioritize measures to prevent SOC loss in the southwest of Heilongjiang Province, where SOC has shown a continuous declining trend historically, and its level in 2023 remains below the critical threshold for crop yields.

Furthermore, the aging agricultural workforce and the limited modern farming skills of smallholders may threaten the sustainable management of cropland soils in Northeast China.[60,61] Rural-to-urban migration of young people, along with declining fertility rates, has led to a significant shortage of young agricultural laborers in Northeast China. For example, census data show that the agricultural labor force in Heilongjiang Province decreased from 20.07 million in 1978 to 10.47 million in 2022. Meanwhile, the percentage of people working in agriculture over the age of 65 has tripled between 1980 and 2020, reaching ~15% of the population in 2020.[62,63] Older smallholders, familiar with traditional farming practices, may have limited capacity to update their agricultural knowledge due to low education levels.[24] In contrast, the young people in China are not interested in agriculture because of its poor economic gains and harsh working conditions.[64] The lack of young laborers with modern agricultural skills may constrain the agricultural transformation of Northeast China from the labor-intensive smallholder farming to modern agriculture. Besides, the land transfer (defined as the transfer of farmland contractual management rights through rental or subcontracting, following the law) in Northeast China is common due to the outflow of young laborers and the low economic gains of smallholder farming.[65] Despite the gains in agricultural productivity and economic efficiency brought by land transfer policies, contractors often prioritize short-term profits by intensively exploiting black soils, while overlooking the long-term ecological risks.[24]

To address these challenges, promoting digital agriculture offers a viable pathway. Digital agriculture is the application of digital and geospatial technologies, integrating sensing, data analytics, and automation, to enable effective monitoring and management of soil, climate, and genetic resources across field and landscape scales.[66] Compared to the other regions of China, croplands in Northeast China are flatter and less fragmented, and thus, they are more suitable for large-scale mechanical operations.[65] This situation offers a good opportunity for accelerating the agricultural transformation of Northeast China through developing digital agriculture. Digital agriculture has the potential to enhance crop productivity and economic and environmental benefits,[67] and to create new job opportunities for the next generation. Thus, it may attract young people to join modern agricultural production activities, thereby overcoming the shortage of agricultural labor.

For sustainable use of black soils in China through digital agriculture, two additional factors should not be overlooked, because of the complexity of agricultural systems and the costs associated with the adoption of digital agriculture.[68] First, developing dynamic models that integrate multisource and multiscale data to monitor the status of cropland soils across a large areal extent is indispensable,[69,70] as they can track and represent the response of soil properties to external disturbance. The 4D dynamic model developed in this study provides a potential framework for monitoring SOC across large areal extent, since the multisource covariates adopted in this model are readily attainable. The second involves public and private investment in digital agriculture infrastructure, including soil sensors, soil monitoring networks, intelligent agricultural machinery and equipment, and soil information processing platforms,[71] together with demand-side and supply-side policy measures, including taxation and subsidy instruments.[64] Overall, new technologies, supportive policies, and stakeholder participation are essential to realize the protection and sustainable utilization of the non-renewable black soil resource.

Global black soils protection: challenges and perspectives

The findings from China's black soils provide critical insights for global black soils conservation and sustainable management. In this study, extensive soil sampling has enabled a robust modeling of SOC dynamics in China's black soil region. However, many other globally distributed black soil regions (such as the East European Plain), face similar challenges of SOC depletion driven by intensive cultivation, climate change, and inadequate organic carbon replenishment (Figure 7).[3,10] Unlike China, where sampling is extensive, these regions often have sparse soil data, especially in high-latitude areas such as Siberia, which presents a significant obstacle to accurately monitoring SOC changes over time. Although recent advances, such as the 30-meter global SOC data products at five-year intervals from 2000 to 2022 released by Hengl et al. (2026),[72] represent significant progress in SOC monitoring, uncertainties remain high in black soil regions owing to the sparse distribution of samples across these soils in the underlying WoSIS soil profile database. To achieve more precise and comprehensive monitoring of SOC dynamics in global black soil regions, it is imperative to advance international collaboration, promote open data sharing, and substantially expand soil profile databases. These efforts are foundational steps toward safeguarding black soil health and ensuring long-term food security worldwide.

REFERENCES

1. Thaler E.A., Larsen I.J., and Yu Q. (2021). The extent of soil loss across the US Corn Belt. *Proc. Natl. Acad. Sci. USA* **118**:e1922375118. DOI:10.1073/pnas.1922375118
2. Zhang J.B., Sun B., Zhu J.J., et al. (2021). Black soil protection and utilization based on harmonization of mountain-river-forest-farmland-lake-grassland-sandy land ecosystems and strategic construction of ecological barrier. *Bull. Chin. Acad. Sci.* **36**:1155–1164. DOI:10.16418/j.issn.1000-3045.20211010002
3. FAO. (2022). Global Status of Black Soils, Roma. DOI:10.4060/cc3124en
4. Tong Y.X., Angelini M.E., Yigini Y. et al. (2024). Global black soil distribution. *Front. Agric. Sci. Eng.* **11**:271–281. DOI:10.15302/J-FASE-2024567
5. FAO. (2023). A call to protect the world's food basket: Black soils, Roma. https://openknowledge.fao.org/handle/20.500.14283/cc6845en
6. Zhang G.L., Long H., and Yang F. (2024). Understanding the formation time of black soils. *Innov. Geosci.* **1**:100010. DOI:10.59717/j.xinn-geo.2023.100010
7. Lu Y.L., Nakicenovic N., Visbeck M., et al. (2015). Five priorities for the UN sustainable development goals. *Nature* **520**:432–433. DOI:10.1038/520432a
8. Rui Y.C., Jackson R.D., Cotrufo M.F., et al. (2022). Persistent soil carbon enhanced in Mollisols by well-managed grasslands but not annual grain or dairy forage cropping systems. *Proc. Natl. Acad. Sci. USA* **119**:e2118931119. DOI:10.1073/pnas.2118931119
9. Liu B.Y., Zhang G.L., Xie Y., et al. (2021). Delineating the black soil region and typical black soil region of northeastern China. *Chin. Sci. B-Chin.* **66**:96–106. DOI:10.1360/TB-2020-0178
10. Li R., Hu W.Y., Jia Z.J., et al. (2025). Soil degradation: A global threat to sustainable use of black soils. *Pedosphere* **35**:264–279. DOI:10.1016/j.pedsph.2024.06.011
11. Han X.Z. and Zou W.X. (2018). Effects and suggestions of black soil protection and soil fertility increase in Northeast China. *Bull. Chin. Acad. Sci.* **33**:206–212. DOI:10.16418/j.issn.1000-3045.2018.02.011
12. Li B.G., Liu Z., Huang F. et al. (2021). Ensuring national food security by strengthening high-productivity black soil granary in Northeast China. *Bull. Chin. Acad. Sci.* **36**:1184–1193. DOI:10.16418/j.issn.1000-3045.20210706003
13. Brinkman H. and Hendrix J.C.S. (2011). Food insecurity and violent conflict: Causes, consequences, and addressing the challenges. Occasional Paper 24, World Food Programme, Rome. DOI:10.13140/2.1.3379.2003
14. Garnett T., Appleby M.C., Balmford A., et al. (2013). Sustainable intensification in agriculture: Premises and policies. *Science* **341**:33–34. DOI:10.1126/science.1234485
15. Laber M., Klimek P., Bruckner M., et al. (2023). Shock propagation from the Russia–Ukraine conflict on international multilayer food production network determines global food availability. *Nat. Food* **4**:508–517. DOI:10.1038/s43016-023-00771-4
16. Lu Y.L., Jenkins A., Ferrier R.C., et al. (2015). Addressing China's grand challenge of achieving food security while ensuring environmental sustainability. *Sci. Adv.* **1**:e1400039. DOI:10.1126/sciadv.1400039
17. Lu Y.L., Zhang Y.Q., Cao X.H., et al. (2019). Forty years of reform and opening up: China's progress toward a sustainable path. *Sci. Adv.* **5**:eaau9413. DOI:10.1126/sciadv.aau9413
18. Lal R. (2004). Soil carbon sequestration impacts on global climate change and food security. *Science* **304**:1623–1627. DOI:10.1126/science.1097396
19. Minasny B., Malone B.P., McBratney A.B., et al. (2017). Soil carbon 4 per mille. *Geoderma* **292**:59–86. DOI:10.1016/j.geoderma.2017.01.002
20. Qiao L. Wang X.H., Smith P., et al. (2022). Soil quality both increases crop production and improves resilience to climate change. *Nat. Clim. Change* **12**:574–580. DOI:10.1038/s41558-022-01376-8
21. Ma Y.Q., Woolf D., Fan M.S., et al. (2023). Global crop production increase by soil organic carbon. *Nat. Geosci.* **16**:1159–1165. DOI:10.1038/s41561-023-01302-3
22. Piao S.L. Fang J.Y., Ciais P., et al. (2009). The carbon balance of terrestrial ecosystems in China. *Nature* **458**:1009–1013. DOI:10.1038/nature07944
23. Fang J.Y., Yu G.R., Liu L.L., et al. (2018). Climate change, human impacts, and carbon sequestration in China. *Proc. Natl. Acad. Sci. USA* **115**:4015–4020. DOI:10.1073/pnas.1700304115
24. Zhao Y.C., Wang M.Y., Hu S.J., et al. (2018). Economics- and policy-driven organic carbon input enhancement dominates soil organic carbon accumulation in Chinese croplands. *Proc. Natl. Acad. Sci. USA* **115**:4045–4050. DOI:10.1073/pnas.1700292114
25. Wang X., Li S.J., Wang L.P., et al. (2023). Effects of cropland reclamation on soil organic carbon in China's black soil region over the past 35 years. *Glob. Change Biol.* **29**:5460–5477. DOI:10.1111/gcb.16833
26. Meng X.T., Bao Y.L., Luo C., et al. (2024). SOC content of global Mollisols at a 30 m spatial resolution from 1984 to 2021 generated by the novel ML-CNN prediction model. *Remote Sens. Environ.* **300**:113911. DOI:10.1016/j.rse.2023.113911
27. Zhou Z.H., Wang C.K., Li Y., et al. (2024). Carbon gain in upper but loss in deeper cropland soils across China over the last four decades. *Proc. Natl. Acad. Sci. USA* **122**:e2422371122. DOI:10.1073/pnas.2422371122
28. Loveland P. and Webb J. (2003). Is there a critical level of organic matter in the agricultural soils of temperate regions: A review. *Soil Tillage Res.* **70**:1–18. DOI:10.1016/S0167-1987(02)00139-3
29. Piao S.L., Ciais P., Huang Y., et al. (2010). The impacts of climate change on water resources and agriculture in China. *Nature* **467**:43–51. DOI:10.1038/nature09364

30. Zhao C., Liu B., Piao S.L., et al. (2017). Temperature increase reduces global yields of major crops in four independent estimates. *Proc. Natl. Acad. Sci. USA* 114:9326–9331. DOI:10.1073/pnas.1701762114
31. Institute of Soil Science, Chinese Academy of Sciences. (1978). Soil Physics and Chemistry Analysis. Shanghai Science and Technology Press. http://opac.stlib.cn/bookInfo_01a0010630.html
32. Hassani A. Azapagic A., and Shokri N. (2020). Predicting long-term dynamics of soil salinity and sodicity on a global scale. *Proc. Natl. Acad. Sci. USA* 117:33017–33027. DOI:10.1073/pnas.2013771117
33. Chen J., Xie E.Z., Peng Y.X., et al. (2025). Four-dimensional modelling reveals decline in cropland soil pH during last four decades in China's Mollisols region. *Geoderma* 453:117135. DOI:10.1016/j.geoderma.2024.117135
34. Xie E.Z., Zhang X., Lu F.Y., et al. (2022). Integration of a process-based model into the digital soil mapping improves the space-time soil organic carbon modelling in intensively human-impacted area. *Geoderma* 7:115599. DOI:10.1016/j.geoderma.2021.115599
35. Zhang X., Xie E.Z., Chen J., et al. (2023). Modelling the spatiotemporal dynamics of cropland soil organic carbon by integrating process-based models differing in structures with machine learning. *J. Soils Sediments* 23:2816–2831. DOI:10.1007/s11368-023-03516-9
36. McBratney A.B., Mendonça Santos M.L., and Minasny B. (2003). On digital soil mapping. *Geoderma* 117:3–52. DOI:10.1016/S0016-7061(03)00223-4
37. Sanchez P.A., Ahamed A., Carré F et al. (2009). Digital soil map of the world. *Science* 325:680–681. DOI:10.1126/science.1175084
38. Minasny B. and McBratney A.B. (2016). Digital soil mapping: A brief history and some lessons. *Geoderma* 264:301–311. DOI:10.1016/j.geoderma.2015.07.017
39. Institute of Tibetan Plateau Research, Chinese Academy of Sciences. (2022). 1 km multi-scenario and multi-model monthly precipitation, temperature, and potential evapotranspiration data for China in 2021–2100. DOI:10.11888/Atmos.tpdc.300558
40. O'Neill B.C., Tebaldi C., van Vuuren D.P., et al. (2016). The scenario model intercomparison project (ScenarioMIP) for CMIP6. *Geosci. Model Dev.* 9:3461–3482. DOI:10.5194/gmd-9-3461-2016
41. Iizumi T. and Sakai T. (2020). The global dataset of historical yields for major crops 1981–2016. *Sci. Data* 7:97. DOI:10.1038/s41597-020-0433-7
42. Berdugo M., Gaitán J.J., Delgado-Baquerizo M., et al. (2022). Prevalence and drivers of abrupt vegetation shifts in global drylands. *Proc. Natl. Acad. Sci. USA* 119:e2123393119. DOI:10.1073/pnas.2123393119
43. Li X.Y., Piao S.L., Huntingford C., et al. (2023). Global variations in critical drought thresholds that impact vegetation. *Natl. Sci. Rev.* 10:nwad049. DOI:10.1093/nsr/nwad049
44. Fong Y.Y., Huang Y., Gilbert P.B., et al. (2017). chngpt: Threshold regression model estimation and inference. *BMC Bioinformatics* 18:454. DOI:10.1186/s12859-017-1863-x
45. Slessarev E.W., Mayer A., Kelly C., et al. (2023). Initial soil organic carbon stocks govern changes in soil carbon: Reality or artifact. *Glob. Change Biol.* 29:1239–1247. DOI:10.1111/gcb.16491
46. Smith J.O., Smith P., Wattenbach M., et al. (2007). Projected changes in the organic carbon stocks of cropland mineral soils of European Russia and the Ukraine, 1990–2070. *Glob. Change Biol.* 13:342–356. DOI:10.1111/j.1365-2486.2006.01297.x
47. Gollany H.T., Rickman R.W., Liang Y., et al. (2011). Predicting agricultural management influence on long-term soil organic carbon dynamics: Implications for biofuel production. *Agron. J.* 103:234–246. DOI:10.2134/agronj2010.0203s
48. Taboada M.A., Micucci F.G., Cosentino D.J., et al. (1998). Comparison of compaction induced by conventional and zero tillage in two soils of the Rolling Pampa of Argentina. *Soil Tillage Res.* 49:57–63. DOI:10.1016/S0167-1987(98)00132-9
49. Zhou G.Y., Xu S., Ciais P., et al. (2019). Climate and litter C/N ratio constrain soil organic carbon accumulation. *Natl. Sci. Rev.* 6:746–757. DOI:10.1093/nsr/nwz045
50. Mishra U., Shelef E., Yang Y.H., et al. (2021). Spatial heterogeneity and environmental predictors of permafrost region soil organic carbon stocks. *Sci. Adv.* 7:eaaz5236. DOI:10.1126/sciadv.aaz5236
51. Villarino S.H., Pinto P., Jackson R.B., et al. (2021). Plant rhizodeposition: A key factor for soil organic matter formation in stable fractions. *Sci. Adv.* 7:eabd3176. DOI:10.1126/sciadv.abd3176
52. He C., Niu J.R., Xu C.T., et al. (2022). Effect of conservation tillage on crop yield and soil organic carbon in Northeast China: A meta - analysis. *Soil Use Manage.* 38:1146–1161. DOI:10.1111/sum.12784
53. Bayer A. and Black A. L. (1994). Quantification of the effect of soil organic matter content on soil productivity. *Soil Sci. Soc. Am. J.* 58:185–193. DOI:10.2136/sssaj1994.03615995005800010027x
54. Díaz-Zorita M., Duarte A., and Grove J.H. (2002). A review of no-till systems and soil management for sustainable crop production in the subhumid and semiarid Pampas of Argentina. *Soil Tillage Res.* 65:1–18. DOI:10.1016/S0167-1987(01)00274-4
55. Dutta K., Schuur E.A.G., Neff J.C. et al. (2006). Potential carbon release from permafrost soils of Northeastern Siberia. *Glob. Change Biol.* 12:2336–2351. DOI:10.1111/j.1365-2486.2006.01259.x
56. Wang X.W., Song C.C., Sun X.X., et al. (2013). Soil carbon and nitrogen across wetland types in discontinuous permafrost zone of the Xiao Xing'an Mountains, northeastern China. *Catena* 101:31–37. DOI:10.1016/j.catena.2012.09.007
57. Wang J.K., Xu X.R., Pei J.B., et al. (2021). Current situations of black soil quality and facing opportunities and challenges in Northeast China. *Chin. J. Soil Sci.* 52:695–701. DOI:10.19336/j.cnki.trtb.2021011103
58. Hou J.G. (2021). Science and technology innovation supporting sustainable use of black soil. *Bull. Chin. Acad. Sci.* 36:1123–1126. DOI:10.16418/j.issn.1000-3045.20210929001
59. Jiang M., Wen Y., Sun M., et al. (2021). Thinking and implementation approach of science and technology strategy of well raising black soil. *Bull. Chin. Acad. Sci.* 36:1146–1154. DOI:10.16418/j.issn.1000-3045.20211009001
60. Ge Q.S., Wang J.Y., and Zhu H.Y. (2021). Overall promotion of black soil protection and rural revitalization: Internal logic, main routes and policy suggestions. *Bull. Chin. Acad. Sci.* 36:1175–1183. DOI:10.16418/j.issn.1000-3045.20210805002
61. Peng X.Z. (2011). China's demographic history and future challenges. *Science* 333:581–587. DOI:10.1126/science.1209396
62. Ren C.C., Zhou X.Y., Wang C., et al. (2023). Ageing threatens sustainability of smallholder farming in China. *Nature* 616:96–103. DOI:10.1038/s41586-023-05738-w
63. Liao D., Cui K., and Ke L.J. (2022). A nationwide Chinese consumer study of public interest on agriculture. *npj Sci. Food* 6:32. DOI:10.1038/s41538-022-00147-1
64. Basso B. and Antle J. (2020). Digital agriculture to design sustainable agricultural systems. *Nat. Sustain.* 3:254–256. DOI:10.1038/s41893-020-0510-0
65. Deng O.P., Ran J.Y., Huang S., et al. (2024). Managing fragmented croplands for environmental and economic benefits in China. *Nat. Food* 5:230–240. DOI:10.1038/s43016-024-00938-7
66. Northrup D.L., Basso B., Wang M.Q., et al. (2021). Novel technologies for emission reduction complement conservation agriculture to achieve negative emissions from row-crop production. *Proc. Natl. Acad. Sci. USA* 118:e2022666118. DOI:10.1073/pnas.2022666118
67. Xiao L.J., Wang G.C., Wang E.L., et al. (2024). Spatiotemporal co-optimization of agricultural management practices towards climate-smart crop production. *Nat. Food* 5:59–71. DOI:10.1038/s43016-023-00891-x
68. Yu Q.Y., Hu Q., Wu H., et al. (2025). View from above: Farmland infrastructure and its impacts on agricultural landscapes. *Innov. Geosci.* 3:100107. DOI:10.59717/j.xinn-geo.2024.100107
69. Lin H.H., Zhao H.J., Duan X.W., et al. (2026). Accelerated warming and soil erosion drive topsoil carbon decline across the Tibetan Plateau: A 40-year resampling analysis. *Innov. Geosci.* 4:100165. DOI:10.59717/j.xinn-geo.2025.100165
70. Wang F., Harindintwali J.D., Wei K., et al., (2023). Climate change: Strategies for mitigation and adaptation. *Innov. Geosci.* 1: 100015. DOI: 10.59717/j.xinn-geo.2023.100015
71. Gao S.Q., Hu Z.M., Wang H.S., et al. (2024). Nine-Step Approach of smart agricultural helps grain production reduce costs, increase yield and efficiency. *Bull. Chin. Acad. Sci.* 39:198–209. DOI:10.16418/j.issn.1000-3045.20230811003
72. Hengl T., Consoli D., Tian X., et al. (2026). OpenLandMap-soildb: Global soil information at 30 m spatial resolution for 2000–2022+ based on spatiotemporal Machine Learning and harmonized legacy soil samples and observations. *Earth Syst. Sci. Data* 18:989–1036. DOI:10.5194/essd-18-989-2026

FUNDING AND ACKNOWLEDGMENTS

This work was supported by the National Key Research and Development Program of China (2023YFB3907401); the Strategic Priority Research Program of the Chinese Academy of Sciences (XDA28010101, XDA28010403); the Science and Technology Plan for the Belt and Road Innovation Cooperation Project of Jiangsu Province, China (BZ2023003); the National Natural Science Foundation of China (42201065); and the China Postdoctoral Science Foundation (2022M720149). The funders had no role in study design, data collection and analysis, decision to publish, or preparation of the manuscript.

AUTHOR CONTRIBUTIONS

J.C., W.Y.H., and Y.C.Z. designed the study. J.C., X.H.X., E.Z.X, and Y.C.Z. developed a spatiotemporal dynamic prediction model for soil organic carbon. J.C., W.Y.H., E.Z.X, G.J.Y., L.X.M., D.S.Y., Y.G.Z., and Y.C.Z. conducted large-scale soil surveys and sampling in the field; J.C., W.Y.H., E.Z.X, Y.Z., T.R.Z., and Y.C.Z. wrote the first draft of the paper. Y.X.T., Z.J.J., M.A.T., M.L.T., and Y.C.Z. contributed to the review and editing of the manuscript. All authors contributed to the manuscript and approved the final version.

DECLARATION OF INTERESTS

The authors declare no competing interests.

DATA AND CODE AVAILABILITY

All data are available in the main text or the supplementary information. Additional data and code available from authors upon request.

SUPPLEMENTAL INFORMATION

It can be found online at https://doi.org/10.59717/j.xinn-geo.2026.100213.